Meteorol. Appl. 9, 345–356 (2002) DOI:10.1017/S1350482702003080

Sensitivity of monsoon circulation and precipitation over India to model horizontal resolution and orographic effects

Yihua Wu[1], S Raman[1], U C Mohanty[2] and R V Madala[3]
[1] *Department of Marine, Earth and Atmospheric Sciences, North Carolina State University, NC 27695-8208, USA*
[2] *Center for Atmospheric Sciences, Institute of Technology, New Delhi, 110016, India*
[3] *Science Applications International Corporation, 1710 Goodridge Drive, McLean, Va. 22102, USA*

A triple-nested regional weather prediction model was used to investigate the effects of the model horizontal resolution and orography on southwest monsoon precipitation over India. Numerical experiments with different resolution topography and different horizontal resolution model domains were conducted. Simulation results indicate that both the distribution and intensity of simulated southwest monsoon precipitation over India is highly sensitive to model horizontal resolution and topography. The model with a finer resolution is able to predict mesoscale organization of rainfall over the land mass. Rainfall predicted over the coarse domain is much less than that observed owing to its unrealistic representation of orographic effects and mesoscale forcings. Simulated wind speed, surface pressure, and latent and sensible heat flux distributions are also sensitive to the model resolution. Larger values and more detailed structure of the distribution of the wind speed and latent and sensible heat fluxes are simulated in the finer domains.

1. Introduction

The horizontal model resolution is an essential issue in both short and extended predictions of circulation features and rainfall in regional and global scale models. Some recent related studies are as follows.

(a) Giorgi & Marinucci (1996), in their investigation of the sensitivity of simulated precipitation to model resolution and its implication for climate studies over Europe, found that the precipitation amounts are sensitive to grid point spacing.
(b) Kallos & Kassomenos (1994) found that wind fields for the same region are different when the horizontal grid increment is changed.
(c) Krishnamurti (1990) conducted global forecasts using the Florida State University global spectral models with different spectral resolutions: T21, T31, T42, T63 and T106. His results show that more realistic circulation patterns and precipitation rates over the monsoon region were simulated with higher resolution models.

There are several reasons for the horizontal model resolution to affect mesoscale circulation features and rainfall predictions. First, local effects, or surface forcing, such as those due to topography, large lakes and coastlines, could be missing in the model on account of its coarse horizontal resolution. Second, important sub-grid processes cannot be represented very well in the model with a coarse resolution. Further, almost all physical parameterisations in a numerical model are sensitive to the horizontal resolution of the model. Thus, the mesoscale forcing, dictated by model resolution, plays an important role in the prediction of the monsoon circulation and rainfall over India. Because of the hydrostatic assumption used in large-scale models and the limitations in computing resources and data, the horizontal resolution of the model cannot be increased arbitrarily. However, an optimum horizontal model resolution that provides the best representation of the model physics is always desirable. The objective of this paper is to present numerical model results about the summer monsoon that show the effect of horizontal model resolution and topography on short-range weather forecasts.

Over India the southwest monsoon occurs from June to September every year. The monsoon brings heavy rainfall over the Indian subcontinent. The country receives more than 75% of its annual rainfall during this period (Rao, 1976; Upadhyay, 1995). Orographic convective precipitation occurs along the west coast and northeast sector of India – these also happen to be

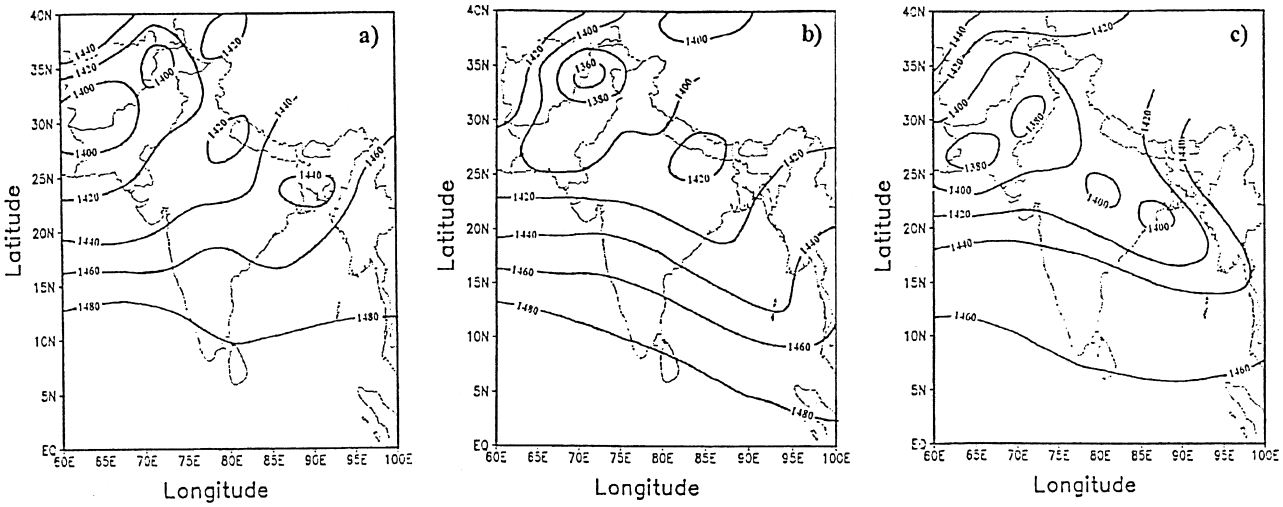

Figure 1. *Observed geopotential height (m) at 850 hPa at 0000 UTC on (a) 12 June 1988, (b) 13 June 1988 and (c) 14 June 1988.*

the regions of heavy monsoon rainfall. The analysis by Krishnamurti *et al.* (1983) shows that maximum rainfall rate along the west coast of India could be as high as about 200 mm d^{-1}, with individual episodes up to 500 mm d^{-1}. It is recognized that the heavy rainfall over the Indian subcontinent during the summer monsoon is mainly due to organized mesoscale convection and localised orographic barriers. During 12–14 July 1988, an active monsoon circulation with a rainfall rate of more than 100 mm d^{-1} was observed along the west coast and over the central and northern regions of India. The rainfall was associated with a mesoscale low pressure system over the monsoon trough region. Much of this rainfall is on the mesoscale and hence this case provides an ideal opportunity to investigate the sensitivity of predicted circulation features and rainfall to the model horizontal resolution and topography.

2. Synoptic overview

During the summer monsoon season, a semi-permanent feature known as the monsoon trough develops over northern India and large convective rainfall occurs along the west coast of the country. Usually, the monsoon trough is located along the Gangetic Plains with a northwest–southeast orientation. During the active monsoon period, the monsoon trough extends so that one end lies over the heat low in northwest Rajasthan and the other end over the Bay of Bengal, crossing the entire northern region of India (Rao, 1976). Low-pressure systems often develop over the Bay of Bengal, and intensify into monsoon depressions. Then they move over land along the monsoon trough causing heavy rainfall over India.

During 12–14 July 1988, the monsoon was moderately active over the Indian subcontinent. Figure 1 shows 850 hPa geopotential heights observed at 0000 UTC on 12, 13 and 14 July. At 0000 UTC on 12 July (Figure 1(*a*)), a heat low was located to the northwest of India with a weak monsoon trough developing over the northern region of India. By 0000 UTC on 13 July (Figure 1(*b*)), the heat low had deepened and the monsoon trough over northern India was now stronger than 24 hours previously. By 0000 UTC on 14 July (Figure 1(*c*)), the intensity of the heat low was about the same but its centre had moved about 100 km to the south. While the monsoon trough over northern India became stronger, two low pressure centres developed over the Bay of Bengal and northern India. During the period the low-level southwesterly flow over the Arabian Sea also strengthened.

The observed 24-hour accumulated rainfall distributions ending at 0300 UTC on 13 and 14 July 1988 are shown in Figure 2. The rainfall occurred mainly over two regions. One is the central and northern parts of India; the other is a region along the west coast of India. During this period the maximum rainfall rate over the central and northern regions of India, as well as over the west coast of India, was about 100 to 140 mm day^{-1}. Rainfall over the central and northern regions of India was associated with the passage of a monsoon low pressure system while the rainfall over the west coast was due to the orographic lifting and associated convection. The analysis shows a seaward increase in rainfall along the west coast of India, indicating that the maximum rainfall over this region may be located offshore during this period. However, this analysis is based on data which lack observations over the ocean and only very sparse observations in the Western Ghat Mountain region where heavy rainfall and floods are often reported during monsoon periods. Thus, the rapid development of low pressure systems of mesoscale nature, heavy rainfall, and active monsoon conditions during this period is very interesting and challenging for numerical simulation.

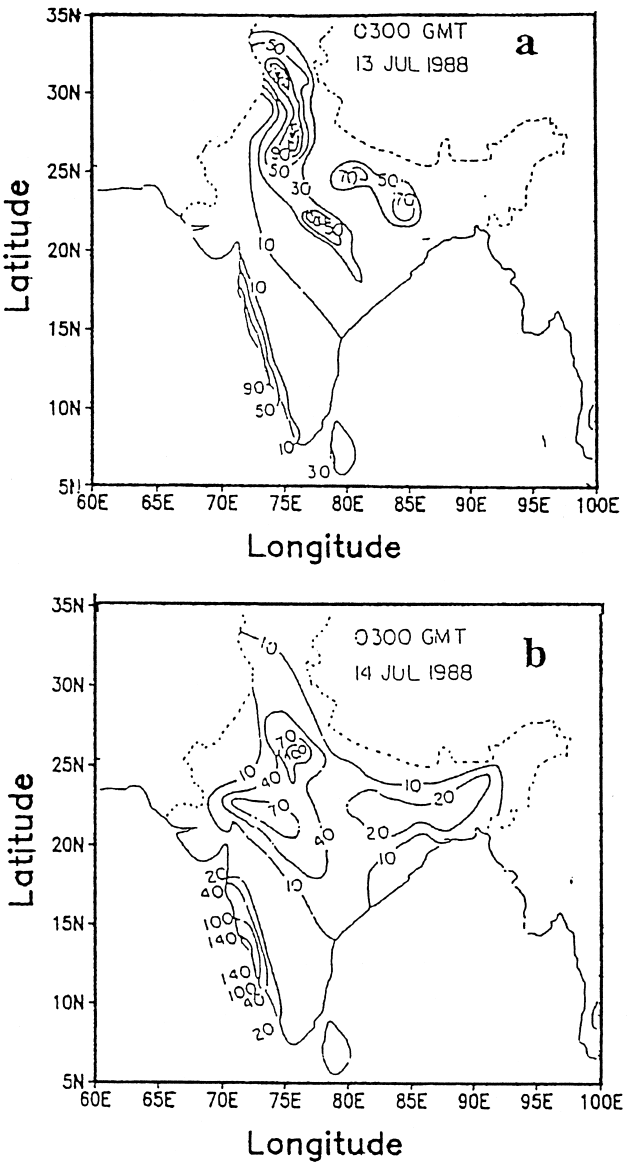

Figure 2. *24-hour accumulated rainfall (mm) ending at 0300 UTC on (a) 13 June 1988 and (b) 14 June 1988.*

3. Model description

The model used in this study is a modified version of the regional weather prediction model originally developed at the Naval Research Laboratory and North Carolina State University (Madala *et al.*, 1987). This model is based on primitive equations in flux form and written in the pressure-based terrain-following σ ($\sigma = p/p_s$) vertical coordinate system. A staggered grid network (Arakawa C-grid) is used for the horizontal differences, with surface pressure, specific humidity, temperature, geopotential and vertical velocity specified at the same horizontal grid points, and zonal and meridional winds between them.

This version contains a capability of multiple nesting with up to three domains running at the same time with one-way interaction. The nesting ratio is 3:1 (i.e. every third grid in a sub-domain is co-located with that in its mother domain). One-way interacting implies that the interior grid points of its mother domain specify the boundary values for a sub-domain with no feedback to the mother domain. The grid size and the time steps are three times less for a sub-domain compared to its mother domain. Lateral boundary conditions are provided using the scheme of Davis (1976, 1983). Any independent variable X can be expressed as: $X = (1–a)\ X_m + a\ X_{b,}$ where X_m represents model-computed values and $X_{b,}$ denotes the boundary values obtained either from observations or from a coarser version of the model. The coefficient, a, ranges from 0 to 1, depending on location of the grid in the boundary zone.

The boundary layer in the model is divided into the surface layer, which is parameterised based on similarity theory (Monin & Yaglom, 1971), and the mixed layer which is parameterised using the E–ε closure scheme (Holt & Raman, 1988). The surface energy budget is performed using the Noilhan & Planton (1989) soil–vegetation parameterisation scheme.

The parameterisation of convective precipitation used in this model is a modified Kuo scheme (Kuo, 1974; Anthes, 1977) which pertains only to columns in which the atmosphere is conditionally unstable and in which the total horizontal moisture convergence exceeds a critical value. A fraction of the total moisture convergence in a column is condensed in cumulus convection and is precipitated out, depending on the mean column relative humidity. The remaining part is retained in the column to increase the humidity of the column and to offset the drying effects of the vertical eddy flux terms.

The parameterisation of non-convective precipitation is based on Manabe *et al.* (1965). Non-convective precipitation occurs in the model when super-saturation is reached on the resolvable scale. Excess moisture precipitates into lower model layers and evaporates or falls to the surface depending on the degree of saturation at those levels.

A split-explicit method is used for time integration in this model. This method allows utilisation of different time steps for the slow-moving Rossby modes and fastest-moving gravity modes in the prognostic equations. A smaller time step is used for the first and second fast-moving gravity modes while a larger time step is used for all other modes. More details about this method as well as the basic structure of the model are given in Madala *et al.* (1987).

4. Model setup and experiments

The nested model domains used for this work are shown in Figure 3.

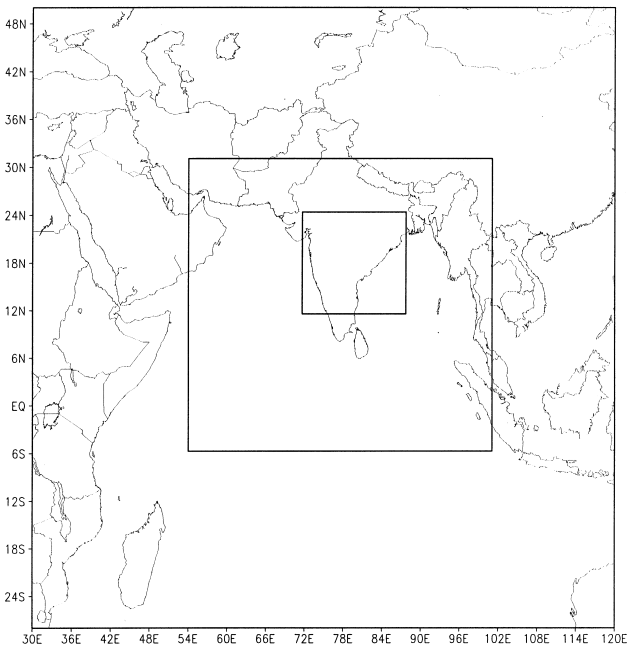

Figure 3. *Physical domains used in the model.*

(a) The coarse resolution domain (CR) is of 8580 × 9900 km^2 size (61 × 53 grid points) and covers most of the monsoon region.
(b) The middle resolution domain (MR) has a size of 5280 × 3960 km^2 (97 × 73 grid points) and encompasses the Indian subcontinent and its surrounding oceans.
(c) The innermost fine resolution domain (FR) is located over the middle region of India, with a size of 1320 × 1980 km^2 (109 × 73 grid points).

Horizontal grid resolutions in CR, MR and FR are 165, 55 and 18 km, respectively. The vertical structure includes 16 σ levels with the model top at about 50 hPa. Eight levels are within the lowest 2 km with a finer resolution at lower levels, and eight equally spaced levels ($\Delta\sigma = 0.1$) above 2 km.

The topography was obtained from the navy 10-minute (18 km) global topography at:

http://www/scd/ucar.edu/catalogs/free.html

The same site provided the sea surface temperatures for the 1 degree resolution global climatological values on a ten-year average for the month of July.

The initial values for the model simulation (wind components, temperature, water vapour mixing ratio and surface pressure) are interpolated from the European Centre for Medium-Range Weather Forecasts (ECMWF) operational analyses at 0000 UTC on 12 July 1988 over a horizontal resolution of about 200 km (1.875° latitude/longitude resolution). Lateral boundary conditions (X_b) for the CR grid points are obtained through a linear interpolation in time step from the ECMWF analyses, while X_b for MR and FR are obtained from the corresponding mother domains. At the model bottom and top, the boundary condition for vertical velocity (ω) is assumed to be zero.

In order to examine the impact of horizontal resolution and topography on the numerical simulation of monsoon circulation features and precipitation, two numerical experiments were conducted. As discussed above, being a triple-nested model with horizontal resolution of CR of 165 km to FR of 18 km, each experiment was built up with three different horizontal resolutions. In order to consider the impact of topography, which is naturally associated with horizontal resolution, different topographies were used for the two experiments.

In the first experiment, the high resolution 10-minute topography was incorporated in the three model domains. The innermost FR domain captures exact high-resolution 10-minute topography since model domain and topography resolution are identical. Over the MR and CR domains, the area-averaged smooth topography at a resolution of 55 km and 165 km respectively were used. The original 10-minute topography in three different horizontal domains is illustrated in Figure 4. As expected, the topography over the FR domain can capture a more detailed structure of peaks and valleys with strong horizontal gradient while over the CR domain very smooth topography with small horizontal gradients are found.

In the second experiment, for all three model domains, the topography of that of the CR domain (i.e. 1.5° latitude/longitude resolution area averaged topography as in Figure 4(*a*)) was used and linearly interpolated to the finer grid points of the MR and FR domains. In this process, the steepness and horizontal gradient of the topography was kept constant over the three model domains.

The model with the three nests was integrated for a total period of 60 hours in both the first and second experiments. Simulated streamlines, wind speed and heat fluxes at 24 h and 48 h, which corresponds to 0000 UTC on 13 July 1988 and 0000 UTC on 14 July 1988 respectively, were analysed. Simulated 24-hour accumulated rainfall ending at 27 h and 51 h, which corresponds to 0300 UTC on 13 July 1988 and 0300 UTC on 14 July 1988 respectively, were also compared with the observations.

To investigate the effects of model horizontal resolution and topography, simulated results from the three different domains in the two experiments were considered only over the same horizontal area with different horizontal resolutions. The area used was 72.0° E to 87.0° E in the east–west direction and from 14.0° N to 24.0° N in the north–south direction (the same as for FR).

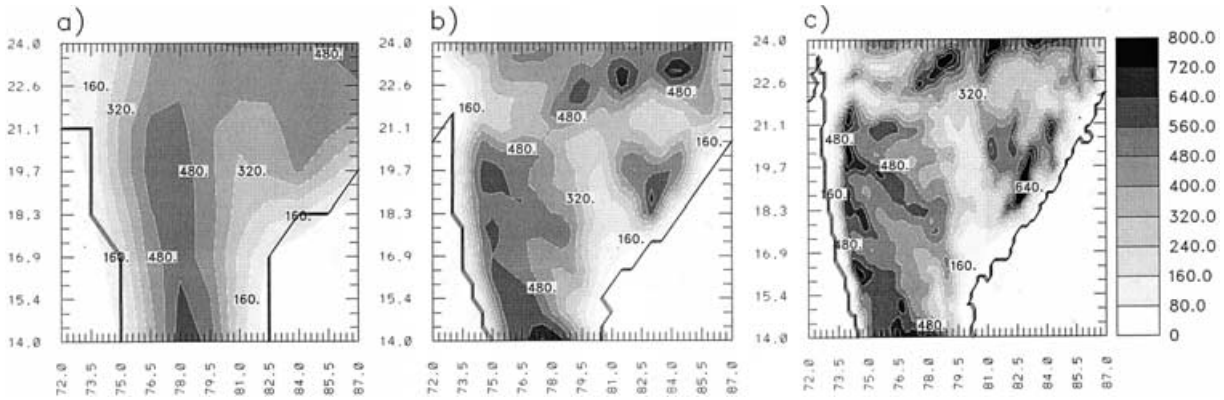

Figure 4. *Topography (m) for the same area (72°–87° E, 14°–24.0° N) in the model for (a) coarse resolution domain (CR), (b) middle resolution domain (MR) and (c) fine resolution domain (FR).*

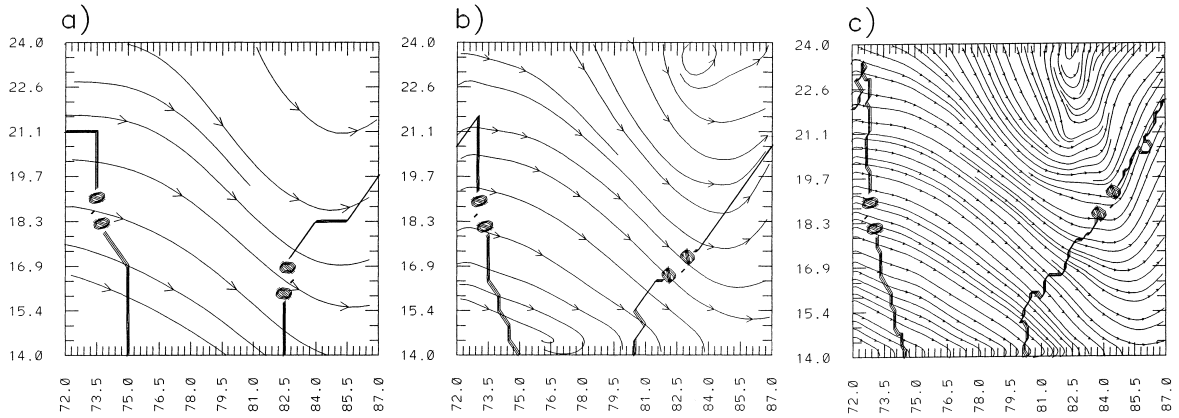

Figure 5. *Streamlines at 850 hPa simulated at 24 h in Experiment 1 for (a) CR, (b) MR and (c) FR.*

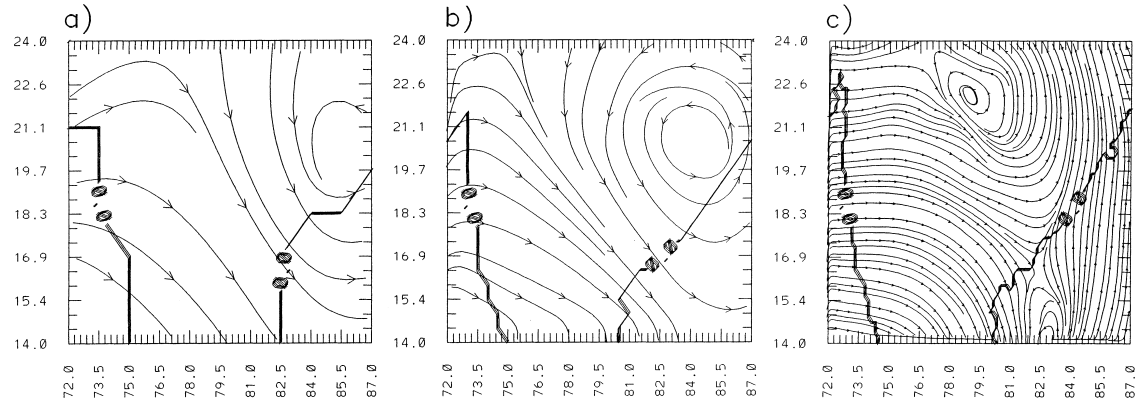

Figure 6. *Streamlines and wind speed (m s^{-1}) at 850 hPa simulated at 48 h in Experiment 1 for (a) streamlines over CR, (b) streamlines over MR and (c) streamlines over FR.*

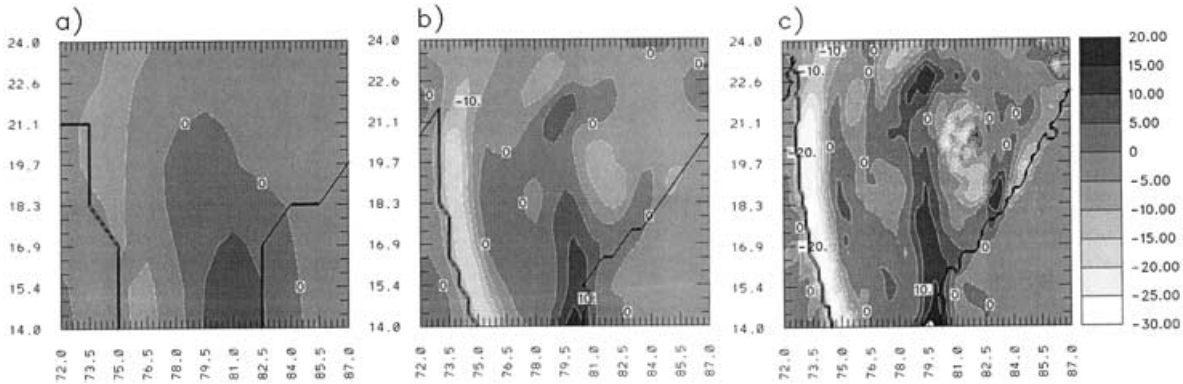

Figure 7. *Near surface vertical velocity (hPa h^{-1}) simulated at 48 h in Experiment 1 for (a) CR, (b) MR and (c) FR.*

5. Experiment 1

This is the control experiment with actual topography for each domain derived from a 10-minute resolution US Navy dataset (the same resolution as that of FR).

5.1. Topography in the three domains

The topography for the same horizontal area from CR, MR and FR is shown in Figure 4. Due to the horizontal resolution effect, differences in topographic structure and height among the three domains are apparent. The Western Ghats are parallel to the west coast of India. They actually extend for about 1600 km in a north–south direction with a mean altitude of 800 m and individual peaks up to 1100 m. The peaks of the Western Ghats are higher and closer to the west coast of India in finer domains than in the coarse domain. The peak along the east coast of India is 700 m in FR, 600 m in MR, but less than 200 m in CR. The highest topography in CR, MR and FR is 610, 731 and 971 m, respectively. The valleys along the east and west coast of India in MR and FR are also missing in CR. Topography in the finer domain captures the features of the Indian peninsula better than that in the coarse domain. However, even the model terrain in FR does not represent the real peaks of the mountains and hence does not fully capture the steepness of the orography.

5.2. Circulation features

Streamlines of the model simulations at 24 h (Figure 5) show that a trough is simulated over the eastern domain. This simulated trough is comparable with that observed in Figure 1(*b*). Comparing the simulations in the three domains, it can be seen that the low pressure system is stronger in the finer domains than in the coarser ones. At 48 h (Figure 6), streamlines of model simulations show that a low pressure centre developed in the region where the trough existed at previous times. The location of the simulated low pressure system is close to the observed one over central India (Figure 1(*c*)). The simulated low pressure system in finer domains is deeper.

General patterns of the simulated winds at 850 hPa (data not shown) are comparable in the three domains. However, the finer the model resolution the more detailed is the structure. The wind patterns for MR and FR show a more consistent cyclonic circulation than that over the CR. As domains become finer, maximum wind speeds get stronger and the structure of the wind distribution around the low pressure system becomes more detailed. Maximum wind speeds over CR, MR, and FR are about 12.5, 15.0 and 22.5 m s^{-1}, respectively. This is due to larger pressure gradients in the finer domains.

Figure 7 shows the simulated vertical velocities (ω) at the first model layer for 48 h. The orographic lifting effect of the Western Ghats is apparent in these fields in all the domains. Rising motion along the west coast of India and sinking motion over southeast India are clearly seen. However, the vertical velocities simulated in the three domains are quite different. Stronger vertical velocity is simulated in the finer domains. The maximum upward motion along the west coast of India at 24 h for CR, MR and FR is about 6, 14 and 22 hPa h^{-1}, respectively. This clearly demonstrates the fact that the simulated vertical velocity is very sensitive to model resolution. Orographic lifting effects become stronger as the domain becomes finer, and, as will be illustrated later, results in stronger rainfall simulation which is found to be closer to that observed.

Simulated latent heat fluxes for the three domains at 24 h and 48 h are examined (data not shown). There are similarities in the simulated results for the three domains: (a) latent heat fluxes are larger over the ocean than over land, and (b) latent heat fluxes are larger over areas where rainfall had occurred over land. However, differences in simulated latent heat fluxes also exist among the three domains with a maximum latent heat flux of 60 W m^{-2} for CR and 120 W m^{-2} for MR as compared to 200 W m^{-2} for FR. Also, a more detailed structure of spatial distribution of latent heat flux is predicted over finer domains.

Simulated sensible heat fluxes for the three domains at 24 h and 48 h are also analysed (data not shown). There are some similarities and some differences among the forecasts for the three domains. Spatial distribution patterns of sensible heat fluxes for the three are similar with the maximum heat flux occurring in the northwest dry desert region with a value of 180 W m^{-2} for FR and 160 W m^{-2} for MR and CR. Thus the maximum values of sensible heat flux are approximately the same for each domain. However, the structure of the spatial distribution of the sensible heat flux shows larger mesoscale gradients as the resolution of the domain becomes finer. This causes stronger mesoscale convergence and more rainfall, as will be discussed below.

5.3. Rainfall on day 1

The observed 24-hour accumulated rainfall ending at 0300 UTC on 13 July 1988 and the corresponding simulated rainfall (model integration from 3 h to 27 h) for the same area are shown in Figure 8. The distribution of rainfall on July 13 (Figure 8(*a*)) occurred over three major regions. The first is along the west coast of India, caused by offshore convections and the interaction of the low-level southwest flow with the Western Ghats; the second, which approximately follows the 80° E line of longitude between 20° N and 24° N, is caused by the monsoon low; and the third is over the northeast region of the domain with a maximum value of 70 mm, again due to the monsoon low.

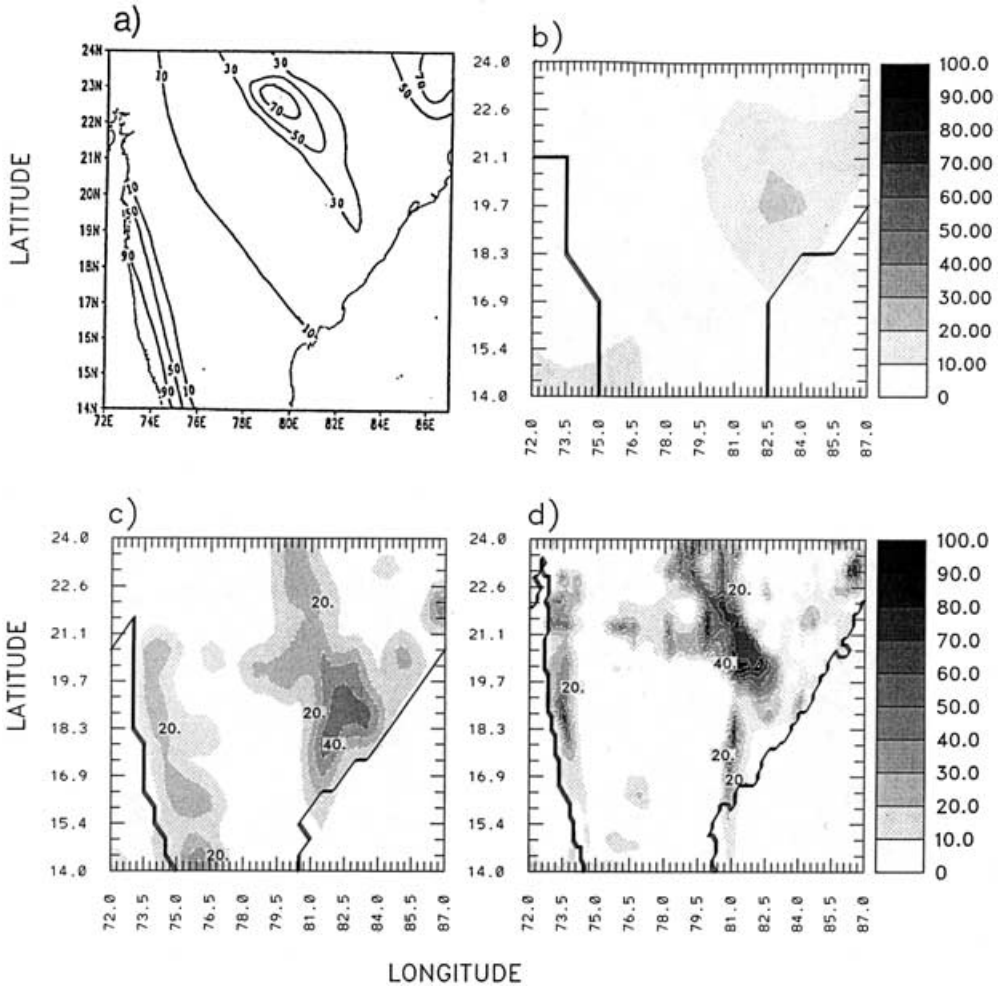

Figure 8. *24-hour accumulated rainfall (mm) observed and simulated in Experiment 1 on day 1 for (a) observed, (b) simulated over CR, (c) simulated over MR and (d) simulated over FR.*

The rainfall pattern simulated in CR (Figure 8(*b*)) does not agree with the observations. Additionally, the rainfall along the west coast is absent in the CR simulation. Obviously, the orographic lifting effect of the Western Ghats could not be represented by the coarse resolution (Δx = 165 km) of the CR domain. Coarser resolution also decreases the non-convective precipitation in the model. The simulated accumulated rainfall of about 20 mm is considerably less than the observed maximum value of 70 mm.

The rainfall distribution pattern is better simulated over MR (Figure 8(*c*)). The simulated inland rainfall amounts are about 30 mm less than the observations, with a maximum value in excess of 40 mm. The location of the simulated maximum rainfall is to the southeast of the observed maximum location. The rainfall along the west coast is better simulated than in CR, although its maximum value is only about 20 mm, less than that observed. The rainfall in the northeast region of the domain is to the south of that observed with smaller values.

Figure 8(*d*) shows the rainfall simulated in FR. The simulation of the rainfall along the west coast is better in this domain compared with the other two. The simulated accumulated rainfall is about 60 mm, which is higher than in CR and MR. The predicted rainfall in the central region agrees well with the observations, with a maximum value of about 90 mm. The rainfall in the northeast region of the domain is also better simulated, with the maximum of 70 mm. It is apparent that the simulated rainfall distribution in the central region is close to the observed in finer domains than in coarser ones. However, simulated accumulated rainfall in the southeast region of the domain is higher than the observed.

5.4. Rainfall on day 2

Observed 24-hour accumulated rainfall ending at 0300 UTC on 14 July and the corresponding simulated rainfall (from 27 h to 51 h) are shown in Figure 9. The observed rainfall (Figure 9(*a*)) was over two regions: along the west coast of India with a maximum of 140 mm, and a widespread region from the central to the northeast of the domain with a maximum of 70 mm.

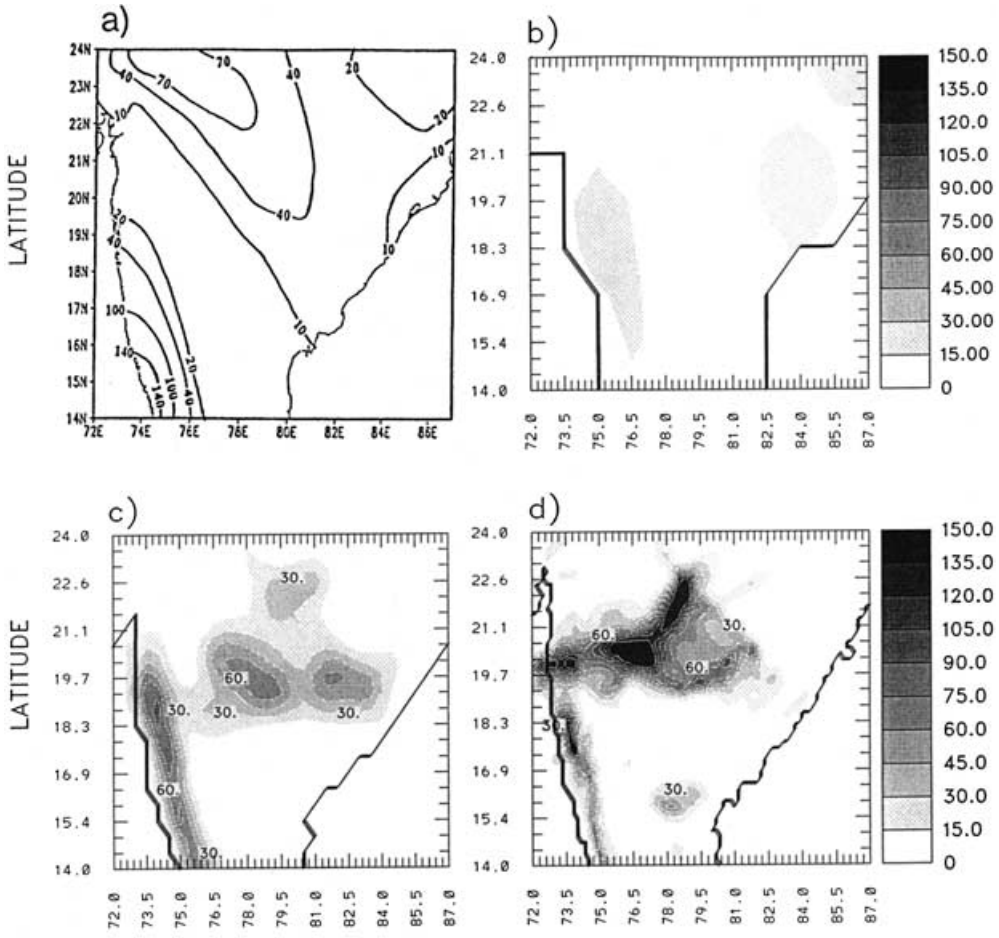

Figure 9. *24-hour accumulated rainfall (mm) observed and simulated in Experiment 1 on day 2 for (a) observed, (b) simulated over CR, (c) simulated over MR and (d) simulated over FR.*

The distribution of the simulated rainfall in CR is illustrated in Figure 9(*b*). This shows that the rainfall along the west coast is only about 15 mm in the CR simulation, much less than the observed. The areas of rainfall in the central and northeast region in CR are much smaller than the observed, and are located to the east of the observed maximum. The simulated maximum is about 15 mm.

The rainfall simulated in MR (Figure 9(*c*)) is better than in CR. In MR the rainfall along the west coast extends from the south to the north with a maximum of about 90 mm, which is less than the observed. Rainfall inland is simulated over a large area with a maximum rainfall of about 60 mm, which is very close to the observed.

The rainfall simulated in the FR is shown in Figure 9(*d*). The distribution of simulated rainfall is similar to that for MR, but with a larger maximum rainfall over both the west coastal region and the inland region. The predicted rainfalls are much closer to the observed values, with the maximum value in the coastal region being about 135 mm, a little less than the observed value. The maximum predicted rainfall inland is about 135 mm, higher than the observations. This could be due to lack of a mesoscale data network over the Indian subcontinent.

6. Experiment 2

In this experiment, the topography for MR and FR was linearly interpolated from that for CR from the previous experiment. Comparisons among the three domains, as well between this experiment and Experiment 1, were made to show the effect of model horizontal resolution and orography.

6.1. Circulation features

The simulated streamlines at 850 hPa at 24 h in Experiment 2 (data not shown) are similar to those in Experiment 1, with a trough simulated over the eastern domain.

At 48 h (Figure 10), the streamlines show that a low pressure centre was simulated over the eastern domain. The low pressure centre in the finer domains is deeper than in coarser ones. This result is also very similar to that in Experiment 1. However, the strength and location of the low pressure system over MR and FR are different from that in the previous experiment, especially over the FR. The low pressure system over FR in Experiment 1 is smaller and weaker than in Experiment 2. Compared with Figure 1(*c*), the low pressure centre

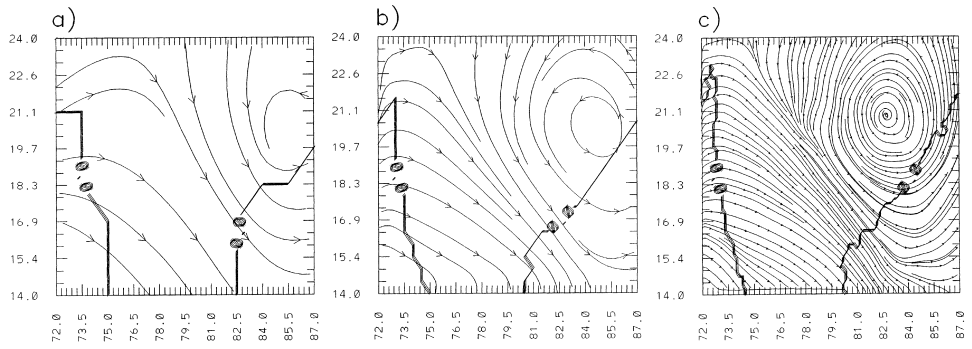

Figure 10. *Streamlines and wind speed (m s^{-1}) at 850 hPa simulated at 48 h in Experiment 2 for (a) streamlines over CR, (b) streamlines over MR and (c) streamlines over FR.*

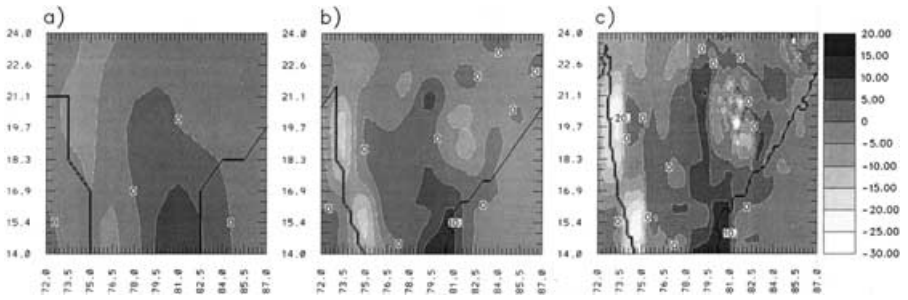

Figure 11. *Near surface vertical velocity (hPa h^{-1}) simulated at 48 h in Experiment 2 for (a) CR, (b) MR and (c) FR.*

simulated is more realistic in Experiment 1 than in Experiment 2. This suggests that the model with higher resolution topography produces better simulation of the low pressure centre.

General patterns of the simulated wind speeds at 850 hPa at 48 h (data not shown) are very similar to those in Experiment 1. The cyclonic circulation simulated over finer domains was more consistent with observations than over coarser domains. Maximum wind speeds are stronger and the structure of the wind distribution around the low pressure system becomes more detailed over finer domains. Little difference in wind speed distribution exists between Experiment 1 and Experiment 2 over CR and MR. However, there is a large difference in FR between the two experiments due to the difference in location and strength of the low pressure system over FR in the two experiments. It may be noted that considerable reduction in horizontal topography gradient introduced in the FR domain is due to the use of smooth topography in Experiment 2.

Simulated vertical velocities at 48 h in Experiment 2 are given in Figure 11. The distribution is very similar to that in Experiment 1, with rising motion along the west coast of India and descending motion in southeast India. Vertical velocities are also stronger in the finer domains. However, vertical velocities over MR and FR in Experiment 2 (Figure 11) are weaker than those in Experiment 1 (Figure 7) because of smoother and flatter topography in Experiment 2. The maximum difference is about 5 hPa h^{-1}.

6.2. Rainfall

Simulated rainfall for day 1 and day 2 in Experiment 2 are given in Figures 12 and 13. As with the results in Experiment 1, the model with finer domains produces better results and the distribution of rainfall shows more detailed structure. Differences in simulated rainfall and its distribution pattern over MR and FR exist between Experiment 1 and Experiment 2 owing to differences in topography. First, the amounts of rainfall over MR and FR in this experiment on day 1 and day 2 are less than those simulated in Experiment 1. On day 1 over MR (Figure 12(*c*)), the maximum rainfall is about the same as in Experiment 1. However, the area of 20 mm along the west coast and inland is much less than that in Experiment 1. On day 1 over FR (Figure 12(*d*)), both the maximum rainfall and the area of 20 mm along the west coast of the country are smaller than those in Experiment 1. The maximum rainfall simulated inland is about the same as in Experiment 1, though the rainfall area is smaller.

On day 2 over MR (Figure 13(*c*)), the maximum rainfall along the west coast is about half that in Experiment 1, but the maximum rainfall inland is about the same. However, the rainfall area is smaller than that in Experiment 1. Comparison of the rainfall on day 2 for FR (Figure 13(*d*)) with the corresponding results in Experiment 1 shows that the maximum rainfall along the west coast is less, the maximum rainfall inland about the same, and the rainfall distribution is different. These results clearly show the effect of topography on monsoon rainfall over the Indian subcontinent. Higher

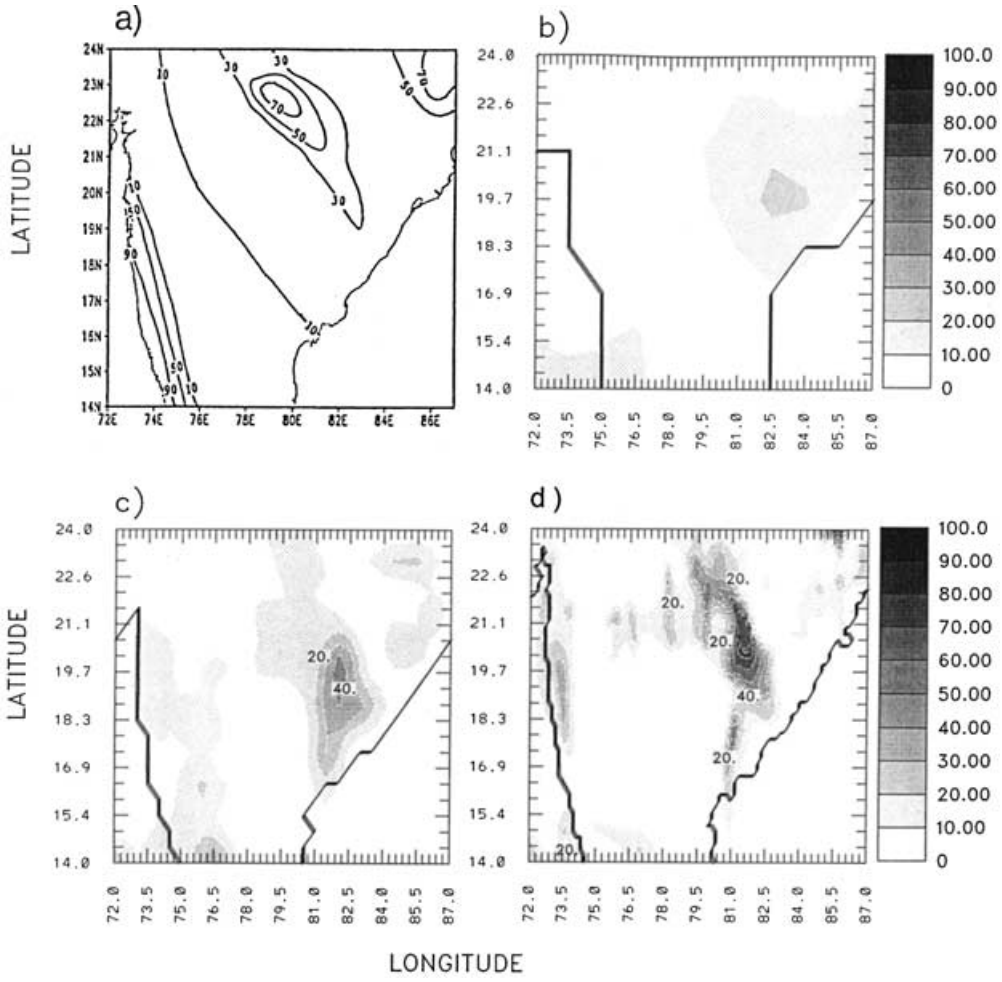

Figure 12. *24-hour accumulated rainfall (mm) simulated in Experiment 2 on day 1 for (a) observed, (b) CR, (c) MR and (d) FR.*

resolution of the topography in the model produces better predictions of rainfall. This agrees with the finding by Jarraud *et al.* (1988) that mountain barrier effects are better represented by the envelope orography and hence the rainfall.

7. Sensitivity of temporal variations of area-averaged parameters

To further show the difference in rainfall among the three domains and the two experiments, area-averaged (72°–87° E and 14°–24° N) rainfall for each hour during the entire 60-hour integration of the model are examined. The minimum, maximum and the mean simulated rainfall for each domain are given in Table 1. It is clearly seen from the table that more rainfall is simulated as the domain becomes finer and as the topography resolution becomes higher.

(a) Area-averaged minimum rainfall rates over both the CR and the MR are zero while it is not over the FR.
(b) Area-averaged maximum and area-time averaged rainfall rates get larger as the domain becomes finer.
(c) Less rainfall was simulated as the topography gradient becomes smaller.

These facts indicate that model resolution and topography gradient play a very important role in the prediction of monsoon rainfall over the Indian subcontinent. There are, at least, three reasons for better simulation results over finer domains in these experiments.

(a) Precipitation estimation in Kuo's scheme depends on horizontal moisture convergence and vertical velocity. Horizontal convergence and vertical velocity are stronger in finer domains. Consequently, more rainfall was simulated over finer domains.

Table 1. *Minimum, maximum and mean simulated rainfall (mm) over the three domains for the same area (72°–87°E, 14°–24°N) in the two experiments.*

Rainfall measure	Experiment 1			Experiment 2		
	CR	MR	FR	CR	MR	FR
Minimum	0.00	0.00	0.12	0.00	0.00	0.11
Maximum	0.61	1.11	2.17	0.61	1.06	2.16
Mean	0.10	0.19	0.95	0.10	0.17	0.91

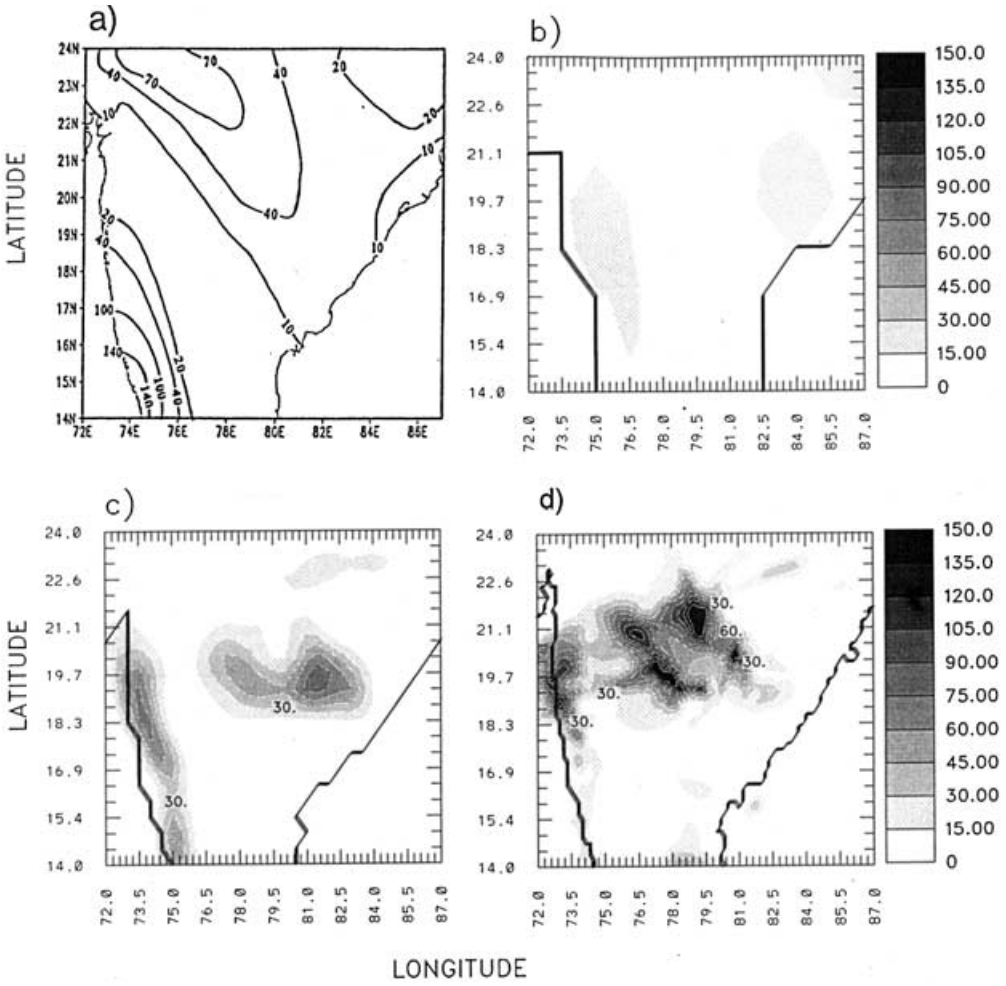

Figure 13. *24-hour accumulated rainfall (mm) simulated in Experiment 2 on day 2 for (a) observed, (b) CR, (c) MR and (d) FR.*

(b) Topography is better presented in finer domains when high-resolution topography is used in the model. The location and structure of the orographic barrier can lead to the generation of sharp and more realistic location-specific precipitation.
(c) Orographic gradients are larger in finer domains when high-resolution topography is used in the model. Larger orographic gradients can lead to stronger Ekman pumping. Therefore, better rainfall results were simulated in finer domains.

It is very difficult to identify explicitly whether the effect of model resolution or topography is larger because the two are closely related. However, an attempt was made by comparing the ratios of the means from the three experiments given in Table 1. The ratios of the means of FR and CR in Experiments 1 and 2 are 9.6 and 9.2, respectively. These values suggest that the effects of model resolution is more important than that of topography.

To further investigate the effect of model resolution on the simulated rainfall and vertical velocity near the surface, corresponding average values for the area (72°–87° E, 14.0°–24° N) over the three domains are given in Figure 14. The following results are found.

(a) The area-averaged vertical velocities indicate that upward motion is stronger in finer domains than in coarser domains (Figure 14(*a*)). The maximum area averages of vertical motions for FR, MR and CR are 3.5, 2.4 and 1.8 hPa h^{-1}, respectively.
(b) Rainfall rates are higher in finer domains (Figure 14(*b*)). The maximum area-averages for FR, MR and CR are 2.0, 1.4 and 0.8 mm h^{-1}, respectively, indicating that simulated rainfall is very sensitive to the horizontal resolution of the model.

8. Conclusions

A triple-nested regional model is used to investigate the effect of the model horizontal resolution and topography on the simulated monsoon flow and the rainfall. The results indicate that the spatial distributions of rainfall are very sensitive to the model horizontal resolution and topography gradient. Larger rainfall rates are simulated as the domain and topography resolution become finer. Vertical velocity, 850 hPa wind speed and their spatial distribution are also sensitive to the model resolution. Stronger 850 hPa wind speeds are simulated in finer resolution nests. Stronger lifting effects due to the mountains are simulated in finer res-

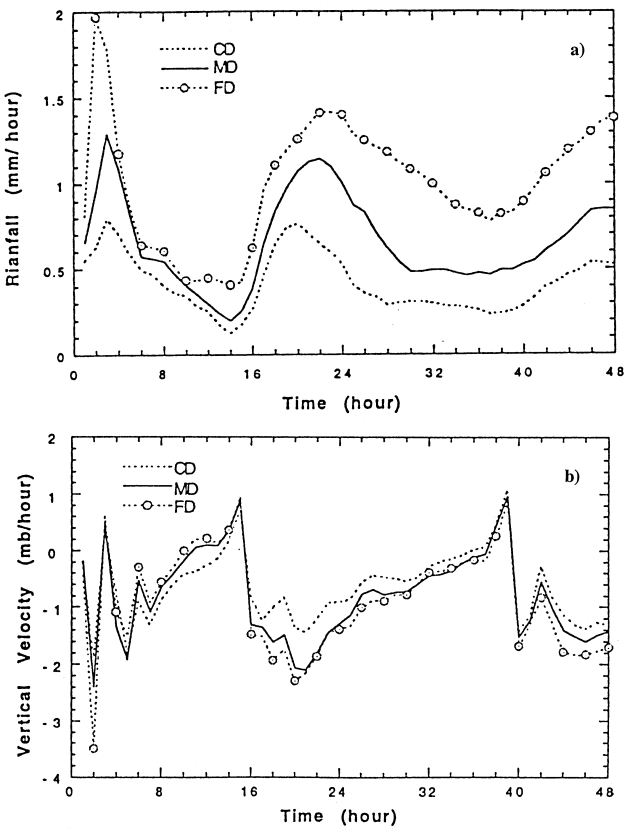

Figure 14. *Temporal variations of area averaged parameters (from 72°–87° E and from 14–24° N) for (a) rainfall and (b) vertical velocity near the surface.*

olution domains. Surface turbulent heat fluxes are also sensitive to the model resolution. The observed precipitation could be simulated better over the innermost nest with a horizontal resolution of 18 km. This study indicates that with the same physics, but with finer horizontal resolution, orographic and mesoscale features can be better simulated. Horizontal resolution appears to improve the area-time mean accumulated rainfall by about one order.

Acknowledgments

This work was supported by the Department of Energy, Atmospheric Sciences Division and the Division of International Progress of the National Science Foundation, the Office of Naval Research and the Naval Research Laboratory, USA. The computation for this work was performed at the North Carolina Supercomputing Center, Research Triangle Park.

References

Anthes, R. A. (1977). A cumulus parameterization scheme utilizing a one-dimensional cloud model. *Mon. Wea. Rev.*, **105:** 207–286.

Davies, H. C. (1976). A lateral boundary formulation for multi-level prediction models. *Q. J. R. Meteorol. Soc.*, **102:** 405–418.

Davies, H. C. (1983). Limitations of some common lateral boundary schemes used in regional NWP models. *Mon. Wea. Rev.*, **111:** 1002–1012.

Giorgi, F. & Marinucci, M. R. (1996). An investigation of the sensitivity of simulated precipitation to model resolution and its implication for climate studies. *Mon. Wea. Rev.*, **124:** 148–166.

Holt, T. & Raman S. (1988). A review and comparative evaluation of multilevel boundary layer parameterizations for first-order and turbulent kinetic energy closure schemes. *Review Geophys.*, **26:** 761–780.

Jarraud, M., Simmons, A. J. & Kanamitsu, M. (1988) Sensitivity of medium-range weather forecasts to the use of an envelope orography. *Q. J. R. Meteorol. Soc.*, **114:** 989–1025.

Kallos, G. & Kassomenos, P. (1994). Effects of the selected domain in mesoscale atmospheric simulations and dispersion calculations. In *Air Pollution Modeling and Its Application X* (eds. S-V. Gryning and M.M. Millan), Plenum Press, New York.

Krishnamurti, T. N. (1990) Monsoon prediction at different resolutions with a global spectral model. *Mausam*, **41:** 234–240.

Krishnamurti, T. N., Cocke, S., Pasch, R. & Low-Nam, S. (1983). Precipitation estimates from rainguage and satellite observations: *Summer MONEX, Dept. of Meteorology, Florida State University*, 377 pp.

Kuo, H. L. (1974). Further studies of the parameterization of the influence of cumulus convection on large-scale flow. *J. Atmos. Sci.*, **31:** 1232–1240.

Madala, R. V., Chang, S. W., Mohanty, U. C., Madan, S. C., Paliwal, R. K., Sarin, V. B., Holt, T., & Raman, S. (1987). Description of the NAVA Research Laboratory Limited Area Dynamical Weather Prediction Model, *NRL Memo. Rep., No. 5992, Naval Research Laboratory, Washington*, D.C.

Manabe, S., Smagorinsky, J. & Strickler, R. F. (1965). Simulated climatology of a general circulation model with a hydrological cycle. *Mon. Wea. Rev.*, **93:** 769–798.

Noilhan, J. & Planton, S. (1989). A simple parameterization of land surface processes for meteorological models. *Mon. Wea. Rev.*, **117:** 536–549.

Rao, Y. P. (1976). *The Southeast Monsoon*. Indian Meteorological Department Monograph No. 1, Indian Meteorological Department. 367 pp.

Upadhyay, D. S. (1995). *Cold Climate Hydrometeorology*. New Age International (P) Limited, Publishers, New Delhi, India.